

## Excitation of the hydrogen atom by fast-electron impact in the presence of a laser field

Manabesh Bhattacharya, C. Sinha, and N. C. Sil

*Department of Theoretical Physics, Indian Association for the Cultivation of Science,  
Jadavpur, Calcutta 700032, India*

(Received 4 October 1990)

An approach has been developed to study the excitation of a ground-state H atom to the  $n=2$  level under the simultaneous action of fast-electron impact and a monochromatic, linearly polarized, homogeneous laser beam. The laser frequency is assumed to be low (soft-photon limit) so that a stationary-state perturbation theory can be applied as is done in the adiabatic theory. An elegant method has been developed in the present work to construct the dressed excited-state wave functions of the H atom using first-order perturbation theory in the parabolic coordinate representation. By virtue of this method, the problem arising due to the degeneracy of the excited states of the H atom has been successfully overcome. The main advantage of the present approach is that the dressed wave function has been obtained in terms of a finite number of Laguerre polynomials instead of an infinite summation occurring in the usual perturbative treatment. The amplitude for direct excitation (without exchange) has been obtained in closed form. Numerical results for differential cross sections are presented for individual excitations to different Stark manifolds as well as for excitations to the  $n=2$  level at high energies (100 and 200 eV) and for field directions both parallel and perpendicular to the incident electron momentum. Extension to a higher order of perturbation is also possible in the present approach for the construction of the dressed states, and the electron-exchange effect can also be taken into account without any further approximation.

### I. INTRODUCTION

The study of atomic excitation under the simultaneous action of electron and photon has recently been a subject of particular interest, especially because of its importance in the field of plasma heating, gas-breakdown phenomena, and also a knowledge of the population of metastable states. The availability of intense laser radiation in a wide range of frequencies has now opened the possibility for measurements of such joint excitation processes of atoms.

A major difficulty in the theoretical investigation of such a problem is to construct the proper dressed atomic excited-state wave functions in the presence of a laser field especially when the target atom has degenerate eigenstates. Specifically, while dealing with the target H atom, one has to be very careful about the  $l$  degeneracy (a peculiarity of the Coulomb interaction) in the excited-state wave functions. In fact, the laser-assisted inelastic electron-atom collisional processes have been studied by several theoretical workers [1–3] in different approaches. Most of the works are done for the weak field using perturbative treatment. In a recent work, Francken *et al.* [4] have investigated such an excitation process of atomic hydrogen by fast electrons in the presence of a laser field. They constructed the “dressed” excited-state wave function by using first-order perturbation theory in the same fashion as was done for the elastic case [5]. But the occurrence of the energy difference term in the denominator of the expression for the dressed wave function [see Ref. 4, Eq. (2)] makes the evaluation of the term very sensitive for the inelastic case. In fact, the denominator sometimes happens to be almost zero except for the laser frequency

term which is a very small quantity. Obviously, this problem which arises due to the degeneracy of the H atom does not come into the picture for the elastic case. Thus, the accuracy of the calculations dealing with such wave functions may be questioned.

In this work, we have proposed an elegant way of constructing the dressed excited-state wave functions using the parabolic coordinate system. This method is free from the above-mentioned difficulties and takes proper account of the degeneracy problem. Although our method can be extended to take account of the Stark effect to higher orders, we have retained only the effect of first-order perturbation in the present calculation.

With this dressed wave function, we have developed a suitable approach to calculate the excitation cross sections of the target H atom under joint electron-photon interaction. The salient feature of the present method is that the direct excitation amplitude has been obtained in a closed analytic form.

### II. THEORY

We consider excitation of the H atom by fast-electron impact from the ground state to an excited state ( $n=2$ ) in the presence of a single mode, linearly polarized, homogeneous laser field represented by (classically)  $\epsilon(t)=\epsilon_0\sin\omega t$ . The corresponding vector potential in Coulomb gauge is given by  $\mathbf{A}(t)=\mathbf{A}_0\cos\omega t$  with  $\mathbf{A}_0=c\epsilon_0/\omega$ .

In the present work, we have developed an elegant method to construct the dressed atomic wave functions in the presence of a laser field assuming the angular frequency ( $\omega$ ) of the laser field to be small compared to unity so

that the stationary-state perturbation theory in the first order can be applied with sufficient validity.

The Schrödinger wave equation for a hydrogen atom in a uniform electric field is given by

$$\frac{1}{2}\nabla^2\Psi + \left[ E + \frac{1}{r} \right] \Psi = \varepsilon z \Psi, \quad (1)$$

where  $\varepsilon$  is the external field in the direction of the  $z$  axis. Equation (1) has been written in atomic units and we shall work in this unit system from this point on. It is well known that for a H atom in a uniform electric field the separation of variables in the Schrödinger equation is possible in parabolic coordinates and this fact has been utilized conveniently here. Defining the parabolic coordinates  $(\xi, \eta, \Phi)$  by the formulas

$$x = \sqrt{\xi\eta} \cos\Phi, \quad y = \sqrt{\xi\eta} \sin\Phi, \quad z = \frac{1}{2}(\xi - \eta), \quad (2a)$$

or conversely

$$\xi = r + z, \quad \eta = r - z, \quad \phi = \tan^{-1} \left[ \frac{y}{x} \right] \quad (2b)$$

and assuming the eigenfunction  $\Psi$  in the form

$$\Psi = F_1(\xi)F_2(\eta)e^{im\phi}, \quad (3)$$

where  $m$  is the magnetic quantum number, we obtain the following equations for  $F_1$  and  $F_2$  [6]:

$$\frac{d}{d\xi} \left[ \xi \frac{dF_1}{d\xi} \right] + \left[ \frac{1}{2}E\xi + \beta_1 - \frac{m^2}{4\xi} \right] F_1 = \frac{\varepsilon\xi^2}{4} F_1, \quad (4)$$

$$\frac{d}{d\eta} \left[ \eta \frac{dF_2}{d\eta} \right] + \left[ \frac{1}{2}E\eta + \beta_2 - \frac{m^2}{4\eta} \right] F_2 = -\frac{\varepsilon\eta^2}{4} F_2, \quad (5)$$

where the separation parameters  $\beta_1, \beta_2$  are related by

$$\beta_1 + \beta_2 = 1. \quad (6)$$

Now we shall solve the above equations by the perturbation method up to first order. In order to do this, we write

$$F_1 = f_0 + \lambda f_1, \quad F_2 = g_0 + \lambda g_1, \quad (7a)$$

$$E = E_0 + \lambda a, \quad (7b)$$

$$\beta_1 = \beta_{10} + \lambda b, \quad \beta_2 = \beta_{20} - \lambda b, \quad (7c)$$

where  $\lambda = \varepsilon$ .  $\beta_1$  and  $\beta_2$  have been chosen in this manner so that Eq. (6) is satisfied.

Putting Eqs. (7) in Eqs. (4) and (5) and equating the coefficients of similar powers of  $\lambda$  from both sides of Eqs. (4) and (5), we get the following equations:

$$\frac{d}{d\xi} \left[ \xi \frac{df_0}{d\xi} \right] + \left[ \frac{1}{2}E_0\xi + \beta_{10} - \frac{m^2}{4\xi} \right] f_0 = 0, \quad (8a)$$

$$\begin{aligned} \frac{d}{d\xi} \left[ \xi \frac{df_1}{d\xi} \right] + \left[ \frac{1}{2}E_0\xi + \beta_{10} - \frac{m^2}{4\xi} \right] f_1 \\ = \left[ \frac{\xi^2}{4} - \frac{1}{2}a\xi - b \right] f_0, \end{aligned} \quad (8b)$$

$$\frac{d}{d\eta} \left[ \eta \frac{dg_0}{d\eta} \right] + \left[ \frac{1}{2}E_0\eta + \beta_{20} - \frac{m^2}{4\eta} \right] g_0 = 0, \quad (8c)$$

$$\begin{aligned} \frac{d}{d\eta} \left[ \eta \frac{dg_1}{d\eta} \right] + \left[ \frac{1}{2}E_0\eta + \beta_{20} - \frac{m^2}{4\eta} \right] g_1 \\ = \left[ -\frac{\eta^2}{4} - \frac{1}{2}a\eta + b \right] g_0. \end{aligned} \quad (8d)$$

We now introduce in place of  $E_0, \xi, \eta$  the quantities

$$n = \frac{1}{\sqrt{-2E_0}}, \quad \rho_1 = \xi\sqrt{-2E_0} = \xi/n, \quad \rho_2 = \eta/n, \quad (9)$$

whereupon we arrive at the equations for  $f_0$  and  $f_1$ ,

$$\frac{d}{d\rho_1} \left[ \rho_1 \frac{df_0}{d\rho_1} \right] + \left[ -\frac{\rho_1}{4} + n\beta_{10} - \frac{m^2}{4\rho_1} \right] f_0 = 0, \quad (10a)$$

$$\begin{aligned} \frac{d}{d\rho_1} \left[ \rho_1 \frac{df_1}{d\rho_1} \right] + \left[ -\frac{1}{4}\rho_1 + n\beta_{10} - \frac{m^2}{4\rho_1} \right] f_1 \\ = \left[ \frac{n^3\rho_1^2}{4} - \frac{n^2a}{2}\rho_1 - bn \right] f_0, \end{aligned} \quad (10b)$$

and similar equations for  $g_0$  and  $g_1$ .

Using the transformation

$$f_0(\rho_1) = e^{-\rho_1/2} \rho_1^{|m|/2} \omega_{10}(\rho_1), \quad (11)$$

we get for  $\omega_{10}$  the differential equation

$$\rho_1 \omega_{10}'' + (|m| + 1 - \rho_1) \omega_{10}' + n_1 \omega_{10} = 0, \quad (12)$$

with the notation

$$n_1 = n\beta_{10} - \frac{1}{2}(|m| + 1). \quad (13)$$

The solution of Eq. (12) is the well-known associated Laguerre polynomial

$$\omega_{10}(\rho_1) = L_{n_1+|m|}^{|m|}(\rho_1), \quad (14)$$

where  $n_1$  must be a non-negative integer. Similarly, we obtain

$$g_0(\rho_2) \equiv e^{-\rho_2/2} \rho_2^{|m|/2} \omega_{20}(\rho_2), \quad (15)$$

where

$$\omega_{20}(\rho_2) = L_{n_2+|m|}^{|m|}(\rho_2), \quad (16)$$

with

$$n_2 = n\beta_{20} - \frac{1}{2}(|m| + 1). \quad (17)$$

As in the case of  $n_1$ ,  $n_2$  is also a non-negative integer.

In view of Eqs. (6), (13), and (17), it follows that

$$n = n_1 + n_2 + |m| + 1, \quad (18)$$

and thus  $n$  takes only integral values.

To solve Eq. (10b) we take

$$f_1(\rho_1) = e^{-\rho_1/2} \rho_1^{|m|/2} \omega_{11}(\rho_1). \tag{19}$$

Thus, substituting in Eq. (10b), we get

$$\begin{aligned} \rho_1 \omega''_{11} + (|m| + 1 - \rho_1) \omega'_{11} + n_1 \omega_{11} \\ = \left[ \frac{n^3 \rho_1^2}{4} - \frac{n^2 a}{2} \rho_1 - bn \right] \omega_{10}. \end{aligned} \tag{20}$$

The associated Laguerre polynomials  $L_{p+|m|}^{|m|}(x)$  are mutually orthogonal with respect to the weight  $e^{-x} x^{|m|}$  and satisfy the recurrence relation

$$\begin{aligned} x L_{p+|m|}^{|m|}(x) &= \frac{p+|m|}{p+|m|+1} L_{p+|m|+1}^{|m|}(x) \\ &\quad - (2p+|m|+1) L_{p+|m|}^{|m|}(x) \\ &\quad + (p+|m|)^2 L_{p+|m|-1}^{|m|}(x). \end{aligned} \tag{21}$$

The above relation can be obtained from the corresponding relation in Magnus and Oberhettinger [7]. It may be noted here that the associated Laguerre polynomials  $\mathcal{L}_p^{|m|}(x)$  in this reference differ from ours:

$$\mathcal{L}_p^{|m|}(x) = (-1)^{|m|} L_{p+|m|}^{|m|}(x) (p!)^{-1}. \tag{22}$$

Further, it may be mentioned that the recurrence relation [Eq. (21)] can easily be derived from the generating function of the associated Laguerre polynomials.

From Eq. (21) one may write

$$\begin{aligned} x^2 L_{p+|m|}^{|m|}(x) &= A_p L_{p+|m|+2}^{|m|}(x) \\ &\quad + B_p L_{p+|m|+1}^{|m|}(x) + C_p L_{p+|m|}^{|m|}(x) \\ &\quad + D_p L_{p+|m|-1}^{|m|}(x) + E_p L_{p+|m|-2}^{|m|}(x), \end{aligned} \tag{23}$$

where

$$\begin{aligned} A_p &= \frac{(p+1)(p+2)}{(p+|m|+1)(p+|m|+2)}, \\ B_p &= -\frac{2(p+1)(2p+|m|+2)}{(p+|m|+1)}, \\ C_p &= 6p^2 + 6p|m| + 6p + |m|^2 + 3|m| + 2, \\ D_p &= -2(p+|m|)^2(2p+|m|), \\ E_p &= (p+|m|)^2(p+|m|-1)^2. \end{aligned} \tag{24}$$

The form of the right-hand side of Eq. (20) on using the relations (21) and (23) suggests writing  $\omega_{11}$  as

$$\begin{aligned} \omega_{11}(\rho_1) &= PL_{n_1+|m|+2}^{|m|}(\rho_1) + QL_{n_1+|m|+1}^{|m|}(\rho_1) \\ &\quad + RL_{n_1+|m|}^{|m|}(\rho_1) \\ &\quad + SL_{n_1+|m|-1}^{|m|}(\rho_1) + TL_{n_1+|m|-2}^{|m|}(\rho_1). \end{aligned} \tag{25}$$

The coefficients  $P, Q$ , etc., can be calculated by substituting  $\omega_{11}$  in Eq. (25) into Eq. (20), then using the differential equation for the associated Laguerre polynomials [cf. Eq. (12)], and finally equating the coefficients of the different associated Laguerre polynomials from both sides of Eq. (20). We thus obtain

$$\begin{aligned} P &= -\frac{n^3}{8} A_{n_1}, \quad Q = -\frac{n^3}{4} B_{n_1} - \frac{an^2}{2} \frac{(n_1+1)}{(n_1+|m|+1)}, \\ S &= \frac{n^3}{4} D_{n_1} + \frac{an^2}{2} (n_1+|m|)^2, \quad T = \frac{n^3}{8} E_{n_1}. \end{aligned} \tag{26}$$

Regarding the determination  $R$ , the coefficient of  $L_{n_1+|m|}^{|m|}$  occurring in the unperturbed wave function, we note that

$$\begin{aligned} R \left[ \rho_1 \frac{d^2}{d\rho_1^2} L_{n_1+|m|}^{|m|}(\rho_1) + (1+|m|-\rho_1) \frac{d}{d\rho_1} L_{n_1+|m|}^{|m|}(\rho_1) + n_1 L_{n_1+|m|}^{|m|}(\rho_1) \right] \\ = \left[ \frac{n^3}{4} C_{n_1} - \frac{an^2}{2} (2n_1+|m|+1) - bn \right] L_{n_1+|m|}^{|m|}(\rho_1). \end{aligned} \tag{27}$$

Now, in view of Eq. (12) the left-hand side of Eq. (27) turns out to be zero irrespective of the value of  $R$ . Therefore, to maintain the consistency between the two sides of Eq. (27), the right-hand side must vanish. Thus, we get

$$a \frac{n^2}{2} (2n_1+|m|+1) + bn = \frac{n^3}{4} C_{n_1}. \tag{28}$$

For the time being we forget about the arbitrariness in  $R$  and take it as zero for a particular solution.

In a similar fashion, we get

$$g_1(\rho_2) = e^{-\rho_2/2} \rho_2^{|m|/2} \omega_{22}(\rho_2), \tag{29}$$

where

$$\begin{aligned} \omega_{22}(\rho_2) &= P' L_{n_2+|m|+2}^{|m|}(\rho_2) + Q' L_{n_2+|m|+1}^{|m|}(\rho_2) \\ &\quad + R' L_{n_2+|m|}^{|m|}(\rho_2) + S' L_{n_2+|m|-1}^{|m|}(\rho_2) \\ &\quad + T' L_{n_2+|m|-2}^{|m|}(\rho_2), \end{aligned} \tag{30}$$

with

$$\begin{aligned} P' &= \frac{n^3}{8} A_{n_2}, \quad Q' = \frac{n^3}{4} B_{n_2} - \frac{an^2}{2} \frac{(n_2+1)}{(n_2+|m|+1)}, \\ S' &= -\frac{n^3}{4} D_{n_2} + \frac{an^2}{2} (n_2+|m|)^2, \quad T' = -\frac{n^3}{8} E_{n_2}, \end{aligned} \tag{31}$$

$R' = 0$  (for a particular solution),

and

$$\frac{an^2}{2}(2n_2 + |m| + 1) - bn = -\frac{n^3}{4}C_{n_2}. \quad (32)$$

Now, from Eqs. (28) and (32) we get

$$a = \frac{3}{2}n(n_1 - n_2), \quad (33)$$

where use of Eqs. (24) and (18) has been made.

Thus the energy up to first order is given by

$$E = -\frac{1}{2n^2} + \frac{3}{2}\epsilon n(n_1 - n_2) \quad (34)$$

and the solution of Eq. (1) upto first order can now be written as

$$\Psi = N \{ f_0(\rho_1)g_0(\rho_2) + \epsilon_0 \sin \omega t [f_0(\rho_1)g_1(\rho_2) + g_0(\rho_2)f_1(\rho_1) + Mf_0(\rho_1)g_0(\rho_2)] \} e^{im\phi}, \quad (35)$$

where  $N$  is the normalization constant. To maintain the normalization condition of the dressed wave function, we have added a part proportional to the unperturbed solution,  $M$  being the proportionality factor. The arbitrary nature of  $R$  and  $R'$  in Eqs. (25) and (30) has been utilized through  $M$  to satisfy the proper normalization condition.

Now we consider the complete solution up to first order of the time-dependent Schrödinger equation:

$$[H_0 + V(t)]\Phi_{n_1 n_2 m}(\mathbf{r}, t) = i \frac{\partial}{\partial t} \Phi_{n_1 n_2 m}(\mathbf{r}, t). \quad (36)$$

If the frequency of the applied field is sufficiently low, its effect can be treated quasistatically. In other words, the solution at every instant can be regarded as a steady-state

solution appropriate to the instantaneous field.

In the present work, we have assumed the following time dependence of the dressed wave function:

$$\Phi_{n_1 n_2 m}(\mathbf{r}, t) = \Psi \exp \left[ -i \int E(t) dt \right], \quad (37)$$

where  $E$  and  $\Psi$  are given by Eqs. (34) and (35), respectively. This assumption is legitimate when  $\omega$  is small compared to unity. In effect, this approximation amounts to the neglect of a term involving the product  $\epsilon_0 \omega$  in finding the complete solution of the time-dependent Schrödinger equation (36) up to first order. For  $\omega \ll 1$ , the neglect of the term is quite justified as long as the neglected term remains a second-order quantity. This condition is fully satisfied in the choice of  $\omega$  in our present calculation.

Next we concentrate on the particular problem at hand: excitation of the hydrogen atom from the ground state ( $\Phi_{000}$ ) to the  $n=2$  level which contains  $\Phi_{100}$ ,  $\Phi_{010}$ , and  $\Phi_{00\pm 1}$ . We shall now give a brief outline for the specific transition  $\Phi_{000} \rightarrow \Phi_{100}$ .

The transition matrix element for the direct excitation process is given by

$$S_{fi}^d = -i \int_{-\infty}^{+\infty} dt \langle \Psi_f | V | \Psi_i \rangle, \quad (38)$$

where the interaction  $V = 1/r_{12} - 1/r_2$  and

$$\Psi_i = \chi_{k_i}(\mathbf{r}_2, t) \Phi_{000}^d(\mathbf{r}_1, t), \quad (39a)$$

$$\Psi_f = \chi_{k_f}(\mathbf{r}_2, t) \Phi_{100}^d(\mathbf{r}_1, t). \quad (39b)$$

In Eq. (38),  $\chi_{k_i}$  and  $\chi_{k_f}$  are the Volkov solutions representing the nonrelativistic wave functions (normalized to a  $\delta$  function) for the incoming and outgoing electrons of momenta  $\mathbf{k}_i$  and  $\mathbf{k}_f$ , respectively, in the presence of the field and are given by

$$\chi_{k_i}(\mathbf{r}_2, t) = (2\pi)^{-3/2} \exp \left\{ i \left[ \mathbf{k}_i \cdot \mathbf{r}_2 - \mathbf{k}_i \cdot \boldsymbol{\alpha}_0 \sin \omega t - \frac{k_i^2}{2} t - \frac{\epsilon_0^2}{4\omega^2} \left[ t + \frac{\sin 2\omega t}{2\omega} \right] \right] \right\}, \quad (40a)$$

$$\chi_{k_f}(\mathbf{r}_2, t) = (2\pi)^{-3/2} \exp \left\{ i \left[ \mathbf{k}_f \cdot \mathbf{r}_2 - \mathbf{k}_f \cdot \boldsymbol{\alpha}_0 \sin \omega t - \frac{k_f^2}{2} t - \frac{\epsilon_0^2}{4\omega^2} \left[ t + \frac{\sin 2\omega t}{2\omega} \right] \right] \right\}, \quad (40b)$$

with  $\boldsymbol{\alpha}_0 = \boldsymbol{\epsilon}_0 / \omega^2$ . Also,  $\Phi_{000}^d$ ,  $\Phi_{100}^d$  in Eqs. (39) are the dressed ground- and excited-state wave functions of the target hydrogen atom in the presence of the field, given by

$$\Phi_{000}^d(\mathbf{r}_1, t) = \Phi_{000}(\mathbf{r}_1, t) e^{-ia \cdot \mathbf{r}_1}, \quad (41a)$$

$$\Phi_{100}^d(\mathbf{r}_1, t) = \Phi_{100}(\mathbf{r}_1, t) e^{-ia \cdot \mathbf{r}_1}, \quad (41b)$$

where  $\Phi_{000}(\mathbf{r}_1, t)$  and  $\Phi_{100}(\mathbf{r}_1, t)$  can readily be obtained following Eq. (37) and are given by

$$\Phi_{000}(\mathbf{r}_1, t) = \frac{1}{\sqrt{\pi}} e^{-iW_0 t} \left[ e^{-r_1} - \sin \omega t \boldsymbol{\epsilon}_0 \cdot \mathbf{r}_1 \left( 1 + \frac{r_1}{2} \right) e^{-r_1} \right], \quad (42a)$$

$$\Phi_{100}(\mathbf{r}_1, t) = \frac{1}{4\sqrt{\pi}} \exp \left[ -i \left[ W_1 t - 3\epsilon_0 \frac{\cos \omega t}{\omega} \right] \right] e^{-r_1/2} \times \left[ \left[ 1 - \frac{r_1(1 + \cos \theta_1)}{2} \right] + \sin \omega t \epsilon_0 (6 - 3r_1 - 13r_1 \cos \theta_1 - 2r_1^2 + 3r_1^2 \cos^2 \theta_1 + \frac{1}{2}r_1^3 \cos \theta_1 + \frac{1}{2}r_1^3 \cos^2 \theta_1) \right], \quad (42b)$$

where  $W_0$  and  $W_1$  are the unperturbed eigenenergies corresponding to the ground state and the first excited state ( $n=2$ ) of the hydrogen atom, respectively.

The factor  $\exp(-i\mathbf{a}\cdot\mathbf{r}_1)$  in Eq. (41) with  $\mathbf{a}=\mathbf{A}/C=\epsilon/\omega$  arises just to maintain the gauge consistency between the Volkov free wave functions [Eq. (40)] and the dressed target wave functions [Eq. (41)]. It may be noted that the dressed ground-state wave function [Eq. (42a)] following from the present theory is identical with the dressed ground-state wave function given in Schiff [8] and also of Francken *et al.* [6]. Further,  $\Psi_i$  is orthogonal to  $\Psi_f$  up to first order and the unperturbed parts of  $\Phi_{000}^d$  and  $\Phi_{100}^d$  are also orthogonal to their corresponding perturbed parts, as expected.

Following our earlier work, [9] we carry out the time integration in Eq. (38) with the help of the addition theorem of Bessel functions and thus the transition matrix element reduces to the form

$$S_{fi}^d = -i(2\pi)^{-2} \sum_l \delta(E_f - E_i + l\omega) I, \quad (43)$$

where  $l$  is the number of photon exchanged. A positive value of  $l$  means emission of photons while the negative value corresponds to absorption. From the energy conservation relation [cf. Eq. (43)] it follows that

$$k_f^2 = k_i^2 - 2l\omega - \frac{3}{4}, \quad l=0, \pm 1, \pm 2, \dots \quad (44)$$

The integral  $I$  in Eq. (43) is given by

$$I = \int \int d^3r_1 d^3r_2 e^{i(\mathbf{k}_i - \mathbf{k}_f)\cdot\mathbf{r}_2} \times \Phi_{100}^{d*}(\mathbf{r}_1, t) V \Phi_{000}^d(\mathbf{r}_1, t) J_l(\beta) e^{-il\gamma}, \quad (45)$$

where  $J_l(\beta)$  is the Bessel function of order  $l$  and

$$\beta^2 = [(\mathbf{k}_f - \mathbf{k}_i) \cdot \boldsymbol{\alpha}_0]^2 + \left[ \frac{3\epsilon_0}{\omega} \right]^2 \quad (46a)$$

and

$$\gamma = \tan^{-1} \left[ \frac{(\mathbf{k}_f - \mathbf{k}_i) \cdot \boldsymbol{\alpha}_0}{(3\epsilon_0/\omega)} \right]. \quad (46b)$$

This integral has been carried out analytically so that the final transition matrix element is reduced to an exact analytic form.

Transition amplitudes for the other two excited states of the  $n=2$  level may also be deduced following the same procedure as discussed in the previous case. However, one should note a distinction between the cases [ $\Phi_{100}, \Phi_{010}$ ] and [ $\Phi_{00\pm 1}$ ] regarding the energy shift of the unperturbed state. In particular, for the  $\Phi_{00\pm 1}(2P_{\pm 1})$  states, both  $n_1$  and  $n_2$  are zero and there is no energy splitting for this particular pair of states, in contrast to the other two states [ $\Phi_{100}, \Phi_{010}$ ]. Thus, as a result of the external field, the unperturbed  $n=2$  level of atomic hydrogen finally splits into three levels; the first two are shifted above and below by an equal amount and correspond to  $(2S+2P_0) \equiv \Phi_{100}$  and  $(2S-2P_0) \equiv \Phi_{010}$  states, respectively, of the hydrogen atom while the third one corresponding to  $2P_{\pm 1}$  remains unaltered. Now, for sym-

metry reasons, contributions to the differential cross sections due to the  $\Phi_{100}$  and  $\Phi_{010}$  states are found to be identical. Thus, the inelastic differential cross section for the transition from the  $n=1$  to the  $n=2$  level can be written as

$$\left[ \frac{d\sigma}{d\Omega} \right]_{\text{tot}} = 2 \left[ \left[ \frac{d\sigma}{d\Omega} \right]_{100} + \left[ \frac{d\sigma}{d\Omega} \right]_{001} \right]. \quad (47)$$

### III. RESULTS AND DISCUSSIONS

We have computed the excitation cross sections for transition from the ground state to  $n=2$  states of atomic hydrogen by fast-electron impact in the presence of a monochromatic laser field of frequency 0.043 a.u. in the soft-photon limit with two different field strengths,  $\epsilon_0=0.003$  and 0.01 a.u. For the time being, the electron-exchange effect has been neglected.

For calculation, the axis of quantization has been chosen to be the direction of the external field  $\epsilon_0$ . We have studied the above inelastic scattering process for two directions of the polarization vector  $\epsilon_0$  of the laser field: (i)  $\epsilon_0$  is parallel to the incident electron momentum  $\mathbf{k}_i$  and (ii)  $\epsilon_0$  is perpendicular to  $\mathbf{k}_i$  with  $\Phi=0$  ( $\mathbf{k}_f, \mathbf{k}_i$ , and  $\epsilon_0$  are coplanar). The results have been computed for two different energies of the incident electron, viz., 100 and 200 eV.

In Figs. 1(a) and 1(b) we have displayed the curves for the differential cross sections  $(d\sigma/d\Omega)_{\text{tot}}$  [cf. Eq. (47)] corresponding to the excitation of the hydrogen atom from the  $n=1$  to the  $n=2$  level for one photon emission ( $l=+1$ ) at two incident energies, 100 and 200 eV, respectively. Figures 2(a) and 2(b) represent the similar curves but for no photon exchange ( $l=0$ ). In all the figures we have shown results for the angular range  $0^\circ$  to  $60^\circ$ . The numerical values of  $(d\sigma/d\Omega)_{\text{tot}}$  for  $l=0, \pm 1$  with  $\epsilon_0 \parallel \mathbf{k}_i$  and  $\epsilon_0 \perp \mathbf{k}_i$  have been arranged in Table I along with the field-free results for two incident energies, 100 and 200 eV, in the same angular range as in Figs. 1 and 2.

In Fig. 1(a) corresponding to the incident electron energy 100 eV, the curve for  $\epsilon_0=0.003$  a.u. and  $\epsilon_0 \parallel \mathbf{k}_i$  falls monotonically from a maximum value which is much less than the field-free result (see Table I). On the other hand, the similar curve for  $\epsilon_0 \perp \mathbf{k}_i$  starts from a small value, increases up to a maximum, and then falls off smoothly. But as the field strength is increased from  $\epsilon_0=0.003$  a.u. to  $\epsilon_0=0.01$  a.u., the nature of the curves for both  $\epsilon_0 \parallel \mathbf{k}_i$  and  $\epsilon_0 \perp \mathbf{k}_i$  get modified significantly. The stronger field curve for  $\epsilon_0 \parallel \mathbf{k}_i$  starts from a maximum value which is greater than the starting maximum value of the weaker field curve and thereafter falls monotonically up to  $36^\circ$  followed by a number of minima and maxima. The similar curve for  $\epsilon_0 \perp \mathbf{k}_i$  reaches a maximum, starting from a small value, then falls sharply followed by oscillations more in number than in the corresponding parallel case. It may be noted that the first minimum in the stronger field curve for  $\epsilon_0 \perp \mathbf{k}_i$  occurs at a smaller angle than that for  $\epsilon_0 \parallel \mathbf{k}_i$ .

With the increase of the incident energy, the qualitative behavior of the curves for two different field

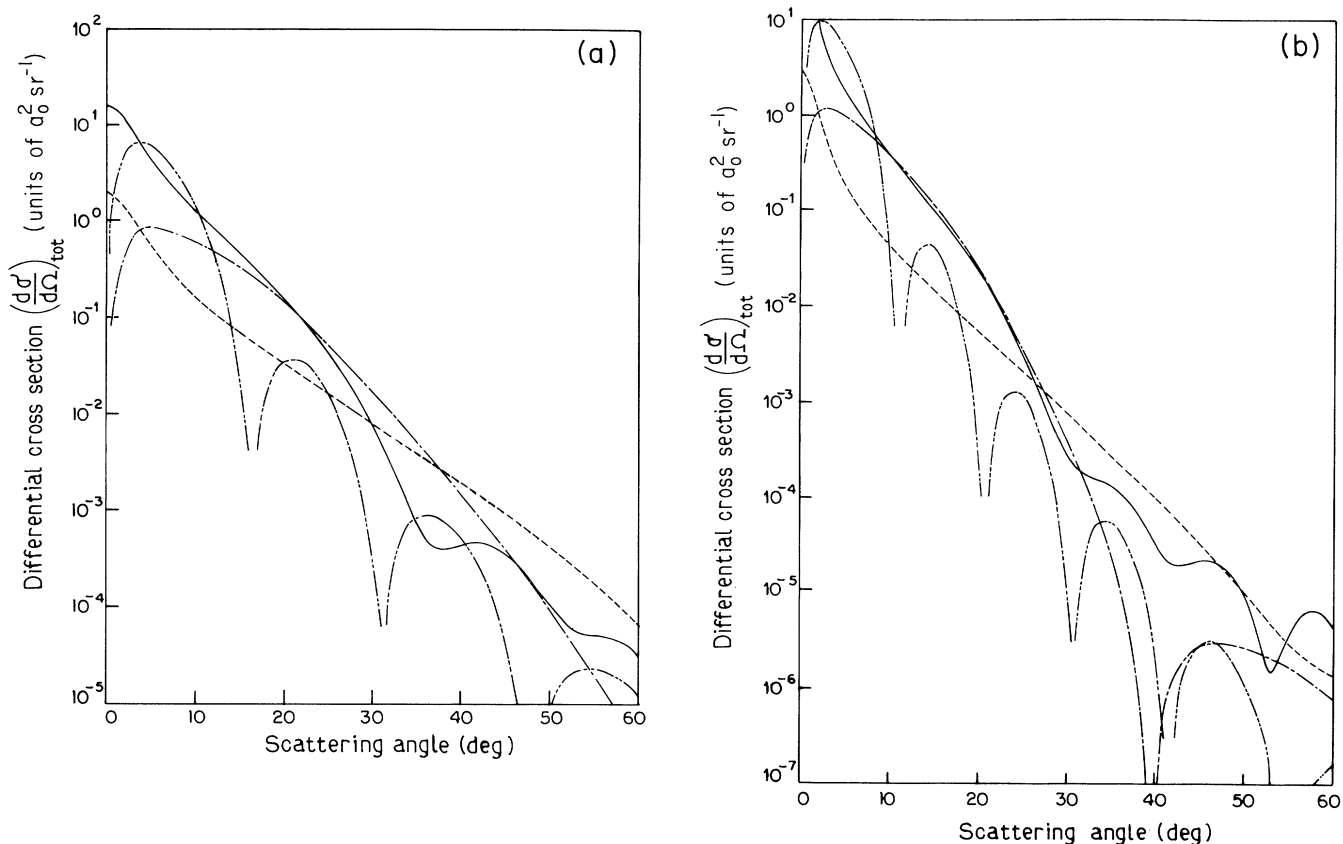


FIG. 1. The differential cross section  $(d\sigma/d\Omega)_{\text{tot}}$  ( $a_0^2 \text{sr}^{-1}$ ) for the excitation of the hydrogen atom to the  $n=2$  level under fast-electron impact in the presence of a laser field with field directions both parallel and perpendicular to the incident electron momentum  $\mathbf{k}_i$  for one-photon emission ( $l=+1$ ) at two incident energies (a)  $E_p=100$  eV and (b)  $E_p=200$  eV. The laser field strengths have been taken as  $\epsilon_0=0.003$  and  $0.01$  a.u. and angular frequency  $\omega=0.043$  a.u.: - - -,  $(d\sigma/d\Omega)_{\text{tot}}$  for  $\epsilon_0=0.003$  a.u. and  $\epsilon_0\parallel\mathbf{k}_i$ ; —, the same for  $\epsilon_0=0.01$  a.u. and  $\epsilon_0\parallel\mathbf{k}_i$ ; - · - · -, the same for  $\epsilon_0=0.003$  a.u. and  $\epsilon_0\perp\mathbf{k}_i$ ; - · · - · ·, the same for  $\epsilon_0=0.01$  a.u. and  $\epsilon_0\perp\mathbf{k}_i$ .

strengths and two polarization directions ( $\epsilon_0\parallel\mathbf{k}_i$  and  $\epsilon_0\perp\mathbf{k}_i$ ) remains more or less the same, as is evident from Fig. 1(b). In the angular range considered, we notice that the weaker field curve for  $\epsilon_0\perp\mathbf{k}_i$  shows a minimum near  $\theta=40^\circ$  instead of a monotonic fall as in the corresponding curve in Fig. 1(a). However, at 100 eV, this minimum, although apparently absent in Fig. 1(a), shows up at a much higher scattering angle (outside the angular range of Fig. 1).

In Fig. 2(a), corresponding to  $l=0$ , the nature of both weaker and stronger field curves for  $\epsilon_0\parallel\mathbf{k}_i$  is similar to the corresponding curves for  $l=1$  in Fig. 1(a). However, the starting values (very close to the field-free results) of the curves in Fig. 2(a) are higher than the starting values of the corresponding curves of Fig. 1(a). The weaker and stronger field curves for  $\epsilon_0\perp\mathbf{k}_i$  in Fig. 2(a) also start from a maximum value whereas in Fig. 1(a), the similar curves start from a small value. Further, the weaker field curve for  $\epsilon_0\perp\mathbf{k}_i$  in Fig. 2(a) has a minimum near  $\theta=34^\circ$  unlike the corresponding curve in Fig. 1(a). However, beyond

the forward region ( $\sim 0^\circ$  to  $4^\circ$ ), the qualitative nature of the curves for  $l=0$  and  $l=+1$  [cf. Figs. 1(a) and 2(a)] seems to be similar when the entire angular region (up to  $180^\circ$ ) is considered. Only the positions of the minima and maxima are different in the two cases. All the curves in Fig. 2(b) follow the same pattern as the corresponding curves in Fig. 2(a) with the increase of the incident energy. However, all the curves become more peaked in the forward direction with increasing incident energy, as expected. Also, in all the curves for stronger field, the fluctuations start earlier, i.e., at comparatively smaller angles, are greater in number, and more closely spaced as the energy is increased. The occurrence of the Bessel functions is responsible for the fluctuations appearing in all the curves for  $l=0$  and  $l=+1$ . The explanation of the difference in the fluctuations of different curves may be as follows:

With increasing energy, the argument of the Bessel function  $\beta$  [cf. Eq. (46a)] increases because of the large momentum transfer in the  $z$  direction, thereby increasing

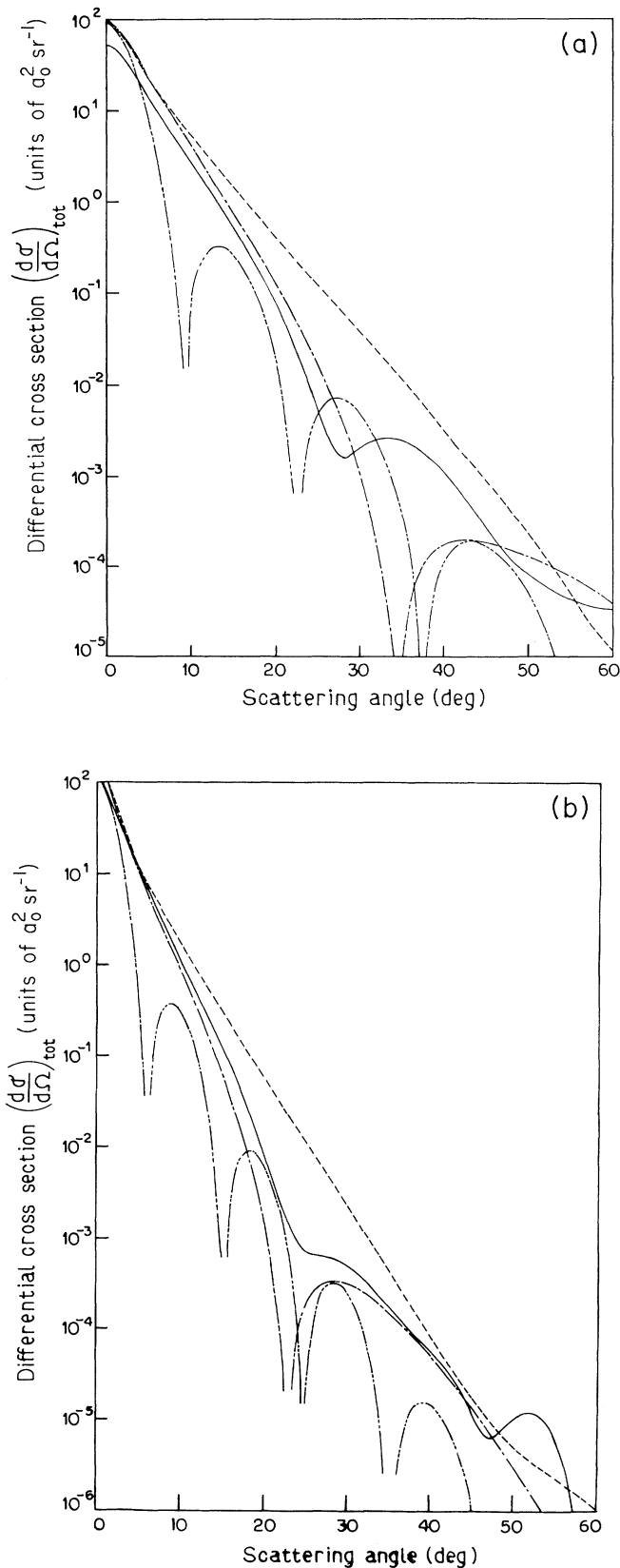


FIG. 2. Same as Fig. 1, but for no-photon exchange ( $l=0$ ).

the number of oscillations in the curves. Further, the occurrence of the field strength  $\epsilon_0$  in  $\beta$  adds to the number of fluctuations with increasing  $\epsilon_0$ , for a given energy. Moreover, for  $\epsilon_0 \perp \mathbf{k}_i$ , the number of fluctuations is larger compared to the  $\epsilon_0 \parallel \mathbf{k}_i$  case because of the enhancement of the span of  $\beta$  arising from the momentum transfer term.

Comparing the curves in Fig. 1(a) ( $l=1$ ) and Fig. 2(a) ( $l=0$ ), it is seen that in the extreme forward direction, the ratio of the cross-section values for stronger and weaker fields for both  $\epsilon_0 \parallel \mathbf{k}_i$  and  $\epsilon_0 \perp \mathbf{k}_i$  in Fig. 1(a) is larger than that in Fig. 2(a) (see also Table I). This indicates that the effect of the external field strength is more prominent in the case of one-photon emission (or absorption) than in the no-photon case. Moreover, irrespective of the field strength, the curve for  $\epsilon_0 \parallel \mathbf{k}_i$  is above the corresponding curve for  $\epsilon_0 \perp \mathbf{k}_i$  in the extreme forward direction for  $l=+1$  [see Fig. 1(a)] while the situation is reversed within the same angular region for  $l=0$  [see Fig. 2(a)]. The above features also hold good for higher energies [cf. Figs. 1(b) and 2(b)].

The curves corresponding to  $l=-1$  (one-photon absorption) cannot be distinguished properly (except for the extreme forward angles; see Table I) from those corresponding to  $l=+1$  in scale, and, as such, we have not shown them.

The values of the individual cross sections  $(d\sigma/d\Omega)_{100}[\Phi_{000} \rightarrow \Phi_{100}]$  and  $(d\sigma/d\Omega)_{001}[\Phi_{000} \rightarrow \Phi_{001}]$  for no-photon exchange ( $l=0$ ) and one-photon emission ( $l=+1$ ) at 100 and 200 eV incident energies have been recorded in Tables II–V considering both field directions  $\epsilon_0 \parallel \mathbf{k}_i$  and  $\epsilon_0 \perp \mathbf{k}_i$ . In Tables II–V we have shown, for all cases, the cross-section results with and without the dressing of the target so that an estimate of the effect of dressing may be obtained. The  $(d\sigma/d\Omega)_{001}$  values (both “no dressing” and “dressing”) at  $\theta=0$  (also at  $\theta=180^\circ$ ) for  $\epsilon_0 \parallel \mathbf{k}_i$  are zero at all incident energies irrespective of the field strength in Tables II–V. The reason lies in the fact that the momentum transfers in  $x$  and  $y$  directions in this case are zero at  $\theta=0$  (and  $\theta=180^\circ$ ). Further, in Tables II and III, the  $(d\sigma/d\Omega)_{001}$  results for  $\epsilon_0 \perp \mathbf{k}_i$  show that the dressing effect becomes zero at  $\theta=0$  (and  $\theta=180^\circ$ ) for all field strengths and at all incident energies. The main reason is that the  $z$  component of the momentum transfer becomes zero at those two angles for  $\epsilon_0 \perp \mathbf{k}_i$ . For the same reason the  $(d\sigma/d\Omega)_{100}$  (without dressing) and  $(d\sigma/d\Omega)_{001}$  (with and without dressing) results in the case of  $\epsilon_0 \perp \mathbf{k}_i$  are zero at  $\theta=0$  (and  $\theta=180^\circ$ ) whatever may be the values of the field strength or incident energies (see Tables IV and V).

It may be noted that, irrespective of the field strength and polarization direction, the individual cross sections  $(d\sigma/d\Omega)_{100}$  and  $(d\sigma/d\Omega)_{001}$  including the dressing of the target are greater than the corresponding values without the dressing effect for  $l=\pm 1$  in contrast to the behavior for  $l=0$ . In other words, the inclusion of the dressing effect enhances the cross sections in the former case while in the latter, it reduces the values. Moreover, in view of Tables II–V, it is seen that the dressing effect is more sensitive with respect to field strength and in-

TABLE I. Differential cross sections  $(d\sigma/d\Omega)_{\text{tot}}(a_0^2 \text{sr}^{-1})$  for the excitation of the H atom to the  $n=2$  level under electron impact in the presence of a laser field of strength  $\epsilon_0=0.003$  and  $0.01$  a.u. at 100 and 200 eV energies for no-photon ( $l=0$ ) and one-photon ( $l=\pm 1$ ) exchanges along with the corresponding field-free results.  $x[y]=x \times 10^y$ .

Field strength (a.u.)	Energy (eV)	Scattering angle (deg)	No field	With field					
				$l=0$		$l=1$		$l=-1$	
				$\epsilon_0 \parallel \mathbf{k}_i$	$\epsilon_0 \perp \mathbf{k}_i$	$\epsilon_0 \parallel \mathbf{k}_i$	$\epsilon_0 \perp \mathbf{k}_i$	$\epsilon_0 \parallel \mathbf{k}_i$	$\epsilon_0 \perp \mathbf{k}_i$
0.003	100	0	9.975[+1]	9.477[+1]	9.974[+1]	1.960	1.003[-2]	2.558	1.042[-2]
		2	6.891[+1]	6.583[+1]	6.767[+1]	1.385	4.808[-1]	1.445	7.740[-1]
		4	3.452[+1]	3.313[+1]	3.249[+1]	7.300[-1]	8.175[-1]	6.115[-1]	1.040
		6	1.767[+1]	1.695[+1]	1.561[+1]	4.054[-1]	8.330[-1]	3.129[-1]	9.592[-1]
		8	9.661	9.236	7.837	2.480[-1]	7.396[-1]	1.878[-1]	8.158[-1]
		10	5.555	5.276	4.036	1.633[-1]	6.156[-1]	1.246[-1]	6.640[-1]
		12	3.302	3.107	2.093	1.131[-1]	4.897[-1]	8.780[-2]	5.207[-1]
		14	2.006	1.865	1.079	8.090[-2]	3.751[-1]	6.417[-2]	3.947[-1]
		16	1.236	1.132	5.471[-1]	5.911[-2]	2.780[-1]	4.793[-2]	2.899[-1]
		18	7.702[-1]	6.919[-1]	2.708[-1]	4.378[-2]	2.000[-1]	3.626[-2]	2.069[-1]
		20	4.840[-1]	4.247[-1]	1.299[-1]	3.270[-2]	1.402[-1]	2.762[-2]	1.439[-1]
		25	1.565[-1]	1.265[-1]	1.668[-2]	1.605[-2]	5.236[-2]	1.415[-2]	5.270[-2]
		30	5.303[-2]	3.780[-2]	1.083[-3]	7.939[-3]	1.752[-2]	7.244[-3]	1.728[-2]
		35	1.893[-2]	1.119[-2]	1.217[-5]	3.908[-3]	5.379[-3]	3.670[-3]	5.188[-3]
		40	7.146[-3]	3.222[-3]	1.746[-4]	1.896[-3]	1.534[-3]	1.826[-3]	1.441[-3]
		45	2.860[-3]	8.780[-4]	1.911[-4]	8.970[-4]	4.058[-4]	8.851[-4]	3.684[-4]
		50	1.213[-3]	2.180[-4]	1.318[-4]	4.076[-4]	9.757[-5]	4.124[-4]	8.438[-5]
		55	5.445[-4]	4.827[-5]	7.601[-5]	1.746[-4]	2.023[-5]	1.818[-4]	1.611[-5]
	60	2.580[-4]	1.178[-5]	4.045[-5]	6.887[-5]	3.137[-6]	7.430[-5]	2.078[-6]	
	200	0	2.156[+2]	2.080[+2]	2.156[+2]	3.020	1.071[-2]	4.181	1.091[-2]
		2	7.467[+1]	7.296[+1]	7.183[+1]	9.177[-1]	1.158	7.607[-1]	1.462
		4	2.283[+1]	2.236[+1]	2.026[+1]	2.813[-1]	1.056	2.052[-1]	1.143
		6	9.069	8.857	7.070	1.292[-1]	8.151[-1]	9.507[-2]	8.538[-1]
		8	4.097	3.977	2.656	7.195[-2]	5.863[-1]	5.482[-2]	6.066[-1]
		10	1.970	1.895	9.988[-1]	4.399[-2]	3.942[-1]	3.478[-2]	4.048[-1]
		12	9.795[-1]	9.306[-1]	3.611[-1]	2.817[-2]	2.487[-1]	2.304[-2]	2.539[-1]
		14	4.971[-1]	4.645[-1]	1.216[-1]	1.847[-2]	1.481[-1]	1.556[-2]	1.504[-1]
		16	2.563[-1]	2.343[-1]	3.662[-2]	1.227[-2]	8.383[-2]	1.060[-2]	8.467[-2]
		18	1.341[-1]	1.192[-1]	9.153[-3]	8.204[-3]	4.532[-2]	7.251[-3]	4.552[-2]
		20	7.116[-2]	6.106[-2]	1.556[-3]	5.514[-3]	2.349[-2]	4.969[-3]	2.346[-2]
		25	1.566[-2]	1.179[-2]	1.754[-4]	2.067[-3]	3.806[-3]	1.941[-3]	3.736[-3]
		30	3.841[-3]	2.335[-3]	3.152[-4]	7.802[-4]	4.537[-4]	7.587[-4]	4.337[-4]
		35	1.053[-3]	4.611[-4]	1.545[-4]	2.907[-4]	2.837[-5]	2.925[-4]	2.533[-5]
		40	3.211[-4]	8.878[-5]	5.159[-5]	1.039[-4]	8.273[-8]	1.087[-4]	1.572[-7]
		45	1.082[-4]	1.776[-5]	1.383[-5]	3.434[-5]	2.670[-6]	3.779[-5]	2.887[-6]
		50	3.997[-5]	4.973[-6]	3.054[-6]	1.027[-5]	2.711[-6]	1.210[-5]	2.780[-6]
55		1.603[-5]	2.212[-6]	5.183[-7]	3.097[-6]	1.654[-6]	3.860[-6]	1.654[-6]	
60	6.930[-6]	1.062[-6]	4.966[-8]	1.424[-6]	8.302[-7]	1.653[-6]	8.151[-7]		
0.01	100	0	9.975[+1]	5.417[+1]	9.956[+1]	1.625[+1]	9.961[-2]	2.330[+1]	1.035[-1]
		2	6.891[+1]	4.034[+1]	5.631[+1]	1.164[+1]	4.761	1.336[+1]	7.691
		4	3.452[+1]	2.145[+1]	1.669[+1]	6.212	6.717	5.726	8.703
		6	1.767[+1]	1.092[+1]	3.307	3.425	5.116	2.916	6.068
		8	9.661	5.689	2.355[-1]	2.042	3.003	1.718	3.425
		10	5.555	3.009	6.963[-2]	1.291	1.398	1.105	1.551
		12	3.302	1.587	2.870[-1]	8.440[-1]	4.790[-1]	7.458[-1]	5.151[-1]
		14	2.006	8.203[-1]	3.103[-1]	5.601[-1]	9.488[-2]	5.146[-1]	9.542[-2]
		16	1.236	4.082[-1]	1.965[-1]	3.719[-1]	4.304[-3]	3.568[-1]	2.390[-3]
		18	7.702[-1]	1.919[-1]	8.043[-2]	2.441[-1]	1.683[-2]	2.455[-1]	1.859[-2]
		20	4.840[-1]	8.303[-2]	1.799[-2]	1.568[-1]	3.544[-2]	1.659[-1]	3.815[-2]
		25	1.565[-1]	5.655[-3]	4.883[-3]	4.408[-2]	1.612[-2]	5.427[-2]	1.554[-2]
		30	5.303[-2]	2.002[-3]	4.824[-3]	8.218[-3]	2.869[-4]	1.273[-2]	1.428[-4]
		35	1.893[-2]	2.435[-3]	3.574[-4]	8.042[-4]	8.366[-4]	1.664[-3]	9.452[-4]
		40	7.146[-3]	1.138[-3]	9.866[-5]	4.293[-4]	5.142[-4]	3.101[-4]	4.738[-4]



TABLE I. (Continued).

Field strength (a.u.)	Energy (eV)	Scattering angle (deg)	No field	With field					
				$l=0$		$l=1$		$l=-1$	
				$\epsilon_0 \parallel \mathbf{k}_i$	$\epsilon_0 \perp \mathbf{k}_i$	$\epsilon_0 \parallel \mathbf{k}_i$	$\epsilon_0 \perp \mathbf{k}_i$	$\epsilon_0 \parallel \mathbf{k}_i$	$\epsilon_0 \perp \mathbf{k}_i$
0.01	100	45	2.860[-3]	2.826[-4]	1.748[-4]	3.534[-4]	4.463[-5]	3.062[-4]	2.647[-5]
		50	1.213[-3]	8.354[-5]	5.184[-5]	1.075[-4]	8.612[-6]	1.360[-4]	1.450[-5]
		55	5.445[-4]	4.500[-5]	2.470[-6]	4.894[-5]	2.440[-5]	5.370[-5]	2.638[-5]
		60	2.580[-4]	3.302[-5]	1.802[-6]	3.205[-5]	1.392[-5]	2.915[-5]	1.239[-5]
200	200	0	2.156[+2]	1.414[+2]	2.154[+2]	2.732[+1]	1.064[-1]	3.997[+1]	1.084[-1]
		2	7.467[+1]	5.751[+1]	4.770[+1]	8.641	1.048[+1]	7.548	1.349[+1]
		4	2.283[+1]	1.808[+1]	4.570	2.689	6.640	2.064	7.493
		6	9.069	6.930	3.613[-2]	1.213	2.743	9.452[-1]	3.019
		8	4.097	2.914	3.032[-1]	6.505[-1]	6.821[-1]	5.311[-1]	7.412[-1]
		10	1.970	1.257	3.233[-1]	3.759[-1]	5.334[-2]	3.239[-1]	5.547[-2]
		12	9.795[-1]	5.360[-1]	1.152[-1]	2.226[-1]	1.347[-2]	2.028[-1]	1.260[-2]
		14	4.971[-1]	2.199[-1]	1.073[-2]	1.313[-1]	4.405[-2]	1.266[-1]	4.517[-2]
		16	2.563[-1]	8.476[-2]	2.228[-3]	7.575[-2]	3.078[-2]	7.747[-2]	3.116[-2]
		18	1.341[-1]	2.985[-2]	8.875[-3]	4.211[-2]	8.794[-3]	4.590[-2]	8.555[-3]
		20	7.116[-2]	9.332[-3]	6.534[-3]	2.221[-2]	4.668[-4]	2.603[-2]	3.584[-4]
		25	1.566[-2]	7.036[-4]	1.479[-5]	3.155[-3]	1.175[-3]	4.745[-3]	1.182[-3]
		30	3.841[-3]	4.971[-4]	2.422[-4]	2.936[-4]	1.280[-5]	5.137[-4]	7.592[-6]
		35	1.053[-3]	1.743[-4]	5.705[-7]	1.361[-4]	5.510[-5]	1.111[-4]	5.581[-5]
		40	3.211[-4]	5.906[-5]	1.486[-5]	3.645[-5]	3.272[-6]	4.032[-5]	2.338[-6]
		45	1.082[-4]	1.221[-5]	1.244[-6]	2.219[-5]	2.791[-6]	2.434[-5]	3.098[-6]
50	3.997[-5]	1.037[-5]	6.126[-7]	9.527[-6]	1.349[-6]	9.514[-6]	1.190[-6]		
55	1.603[-5]	6.099[-6]	6.041[-7]	3.386[-6]	4.685[-9]	3.395[-6]	6.163[-9]		
60	6.930[-6]	1.746[-6]	5.611[-8]	4.290[-6]	1.640[-7]	4.399[-6]	1.828[-7]		

cident electron energy for  $l = \pm 1$  than for the  $l = 0$  case. Of course, the effect of dressing is much more prominent in the forward region, as is evident from Tables II–V.

As for the comparison with other theoretical findings, it should be noted that the dressed atomic states cannot be separated as  $2S$  and  $2P_0$  states, except in the limit of zero field when they correspond to  $2S + 2P_0$  and  $2S - 2P_0$  states. Here, the individual excitation cross section of  $2S$  or  $2P_0$  states in the presence of the field carries no sense. According to the present analysis, the meaningful quantity will be the sum total cross section for the  $n = 2$  level as well as the individual cross sections to different Stark manifold. In fact, we believe that this should be the correct prescription for calculating the excitation probability of the H atom in the presence of a laser field since in this case the orbital angular momentum is no longer a good quantum number. Thus, for a meaningful comparison with some other theoretical results, the sum total cross sections to the  $n = 2$  level are to be compared.

In the work of Francken *et al.* [4] wherein the same problem has been treated without resorting to the parabolic Stark states, cross-section values with one-photon absorption have been presented only for the  $2S$  state for the  $n = 2$  level. So we are not in a position to compare the present total results with their individual  $2S$  cross sections. However, we have also computed the sum total

cross sections with the same parameters as quoted by them for a few angles in the extreme forward direction, viz., at 500 eV and  $\epsilon_0 = 0.0002$ ;  $\omega = 0.043$ , the sum total cross section to the  $n = 2$  level at an angle  $2^\circ$  is  $6.73 \times 10^{-3}$ , whereas the corresponding  $2S$  cross section of Francken *et al.* [4] is  $\sim 8 \times 10^{-4}$  (taken from the curve). It should be pointed out here that because of the particular choice of polar axis, the present results of perpendicular polarization ( $\epsilon_0 \perp \mathbf{k}_i$ ) should correspond to the results of Francken *et al.* [4] with polarization vector  $\epsilon_0 \parallel \mathbf{q}$  at high energy and at extreme forward angles. Since the separation of  $2S$  and  $2P_0$  states is possible in the case when the dressing effect is totally neglected (weak field limit), we have also computed the individual  $2S$ ,  $2P_0$ , and  $2P_{\pm 1}$  cross sections for the above parameters and have found very close agreement with Francken *et al.* [4] for the  $2S$  excitation, which is quite expected.

#### IV. CONCLUSION

The main distinctive aspects of the present method, where the dressed wave function of the hydrogen atom is constructed using parabolic coordinates, are as follows.

(1) The present analysis is free from the difficulty arising from the degeneracy of the excited states, as described in the Introduction.

TABLE II. Differential cross sections  $(d\sigma/d\Omega)_{100}$  and  $(d\sigma/d\Omega)_{001}$  ( $a_0^2 \text{ sr}^{-1}$ ) for the excitations of the H atom to the  $n=2$  level under electron impact in the presence of a laser field of strength  $\epsilon_0=0.003$  a.u. at 100 and 200 eV energies for the no-photon ( $l=0$ ) exchange.  $x[y]=x \times 10^y$ .

Energy (eV)	Scattering angle (deg)	Differential cross sections							
		$\epsilon_0 \parallel \mathbf{k}_i$				$\epsilon_0 \perp \mathbf{k}_i$			
		$\left[ \frac{d\sigma}{d\Omega} \right]_{100}$		$\left[ \frac{d\sigma}{d\Omega} \right]_{001}$		$\left[ \frac{d\sigma}{d\Omega} \right]_{100}$		$\left[ \frac{d\sigma}{d\Omega} \right]_{001}$	
		No dressing	Dressing	No dressing	Dressing	No dressing	Dressing	No dressing	Dressing
100	0	4.857[+1]	4.739[+1]	0	0	4.431[-1]	4.334[-1]	4.943[+1]	4.943[+1]
	2	2.424[+1]	2.366[+1]	9.291	9.257	9.875	9.655	2.421[+1]	2.418[+1]
	4	7.045	6.885	9.720	9.682	9.978	9.720	6.562	6.525
	6	2.422	2.371	6.132	6.106	6.082	5.889	1.942	1.918
	8	1.081	1.060	3.574	3.558	3.386	3.252	6.811[-1]	6.663[-1]
	10	5.893[-1]	5.783[-1]	2.070	2.060	1.846	1.756	2.714[-1]	2.624[-1]
	12	3.633[-1]	3.566[-1]	1.204	1.197	9.946[-1]	9.345[-1]	1.175[-1]	1.121[-1]
	14	2.389[-1]	2.346[-1]	7.024[-1]	6.977[-1]	5.278[-1]	4.891[-1]	5.351[-2]	5.027[-2]
	16	1.617[-1]	1.588[-1]	4.103[-1]	4.071[-1]	2.745[-1]	2.505[-1]	2.499[-2]	2.307[-2]
	18	1.105[-1]	1.085[-1]	2.395[-1]	2.374[-1]	1.392[-1]	1.248[-1]	1.175[-2]	1.064[-2]
	20	7.546[-2]	7.412[-2]	1.396[-1]	1.382[-1]	6.845[-2]	6.008[-2]	5.481[-3]	4.850[-3]
	25	2.827[-2]	2.783[-2]	3.594[-2]	3.544[-2]	9.544[-3]	7.758[-3]	7.132[-4]	5.819[-4]
	30	1.005[-2]	9.949[-3]	9.120[-3]	8.949[-3]	7.598[-4]	5.047[-4]	5.557[-5]	3.664[-5]
	35	3.375[-3]	3.384[-3]	2.265[-3]	2.209[-3]	4.336[-7]	5.793[-6]	3.166[-8]	2.894[-7]
	40	1.056[-3]	1.089[-3]	5.398[-4]	5.219[-4]	5.934[-5]	8.135[-5]	4.363[-6]	5.940[-6]
	45	2.967[-4]	3.261[-4]	1.183[-4]	1.130[-4]	7.792[-5]	8.897[-5]	5.786[-6]	6.591[-6]
	50	6.883[-5]	8.861[-5]	2.181[-5]	2.038[-5]	5.726[-5]	6.133[-5]	4.295[-6]	4.595[-6]
	55	1.041[-5]	2.178[-5]	2.661[-6]	2.359[-6]	3.408[-5]	3.533[-5]	2.581[-6]	2.673[-6]
	60	2.403[-7]	5.863[-6]	5.014[-8]	2.819[-8]	1.849[-5]	1.879[-5]	1.412[-6]	1.435[-6]
200	0	1.064[+2]	1.040[+2]	0	0	4.681[-1]	4.580[-1]	1.073[+2]	1.073[+2]
	2	1.415[+1]	1.384[+1]	2.268[+1]	2.264[+1]	2.292[+1]	2.237[+1]	1.359[+1]	1.354[+1]
	4	1.980	1.940	9.260	9.242	8.948	8.666	1.480	1.463
	6	6.620[-1]	6.496[-1]	3.788	3.779	3.396	3.248	2.943[-1]	2.867[-1]
	8	3.399[-1]	3.336[-1]	1.660	1.655	1.331	1.252	7.944[-2]	7.592[-2]
	10	2.010[-1]	1.972[-1]	7.530[-1]	7.505[-1]	5.172[-1]	4.764[-1]	2.468[-2]	2.304[-2]
	12	1.221[-1]	1.198[-1]	3.469[-1]	3.455[-1]	1.930[-1]	1.732[-1]	8.048[-3]	7.302[-3]
	14	7.357[-2]	7.218[-2]	1.609[-1]	1.601[-1]	6.736[-2]	5.852[-2]	2.593[-3]	2.270[-3]
	16	4.354[-2]	4.274[-2]	7.487[-2]	7.442[-2]	2.128[-2]	1.766[-2]	7.817[-4]	6.522[-4]
	18	2.533[-2]	2.489[-2]	3.496[-2]	3.471[-2]	5.727[-3]	4.418[-3]	2.051[-4]	1.585[-4]
	20	1.452[-2]	1.429[-2]	1.638[-2]	1.624[-2]	1.138[-3]	7.516[-4]	4.024[-5]	2.638[-5]
	25	3.445[-3]	3.421[-4]	2.505[-3]	2.474[-3]	4.664[-5]	8.477[-5]	1.645[-6]	2.952[-6]
	30	7.718[-4]	7.862[-4]	3.879[-4]	3.811[-4]	1.354[-4]	1.522[-4]	4.834[-6]	5.430[-6]
	35	1.591[-4]	1.739[-4]	5.807[-5]	5.662[-5]	7.211[-5]	7.457[-5]	2.612[-6]	2.701[-6]
	40	2.752[-5]	3.711[-5]	7.565[-6]	7.280[-6]	2.502[-5]	2.488[-5]	9.183[-7]	9.138[-7]
	45	3.037[-6]	8.279[-6]	6.462[-7]	6.024[-7]	6.891[-6]	6.668[-6]	2.558[-7]	2.478[-7]
	50	2.964[-8]	2.483[-6]	4.984[-9]	3.209[-9]	1.563[-6]	1.472[-6]	5.857[-8]	5.525[-8]
	55	1.858[-7]	1.079[-6]	2.510[-8]	2.715[-8]	2.758[-7]	2.497[-7]	1.042[-8]	9.456[-9]
	60	3.155[-7]	4.956[-7]	3.469[-8]	3.557[-8]	2.909[-8]	2.392[-8]	1.106[-9]	9.117[-10]

TABLE III. Differential cross sections  $(d\sigma/d\Omega)_{100}$  and  $(d\sigma/d\Omega)_{001}$  ( $a_0^2 \text{ sr}^{-1}$ ) for the excitation of the H atom to the  $n=2$  level under electron impact in the presence of a laser field of strength  $\epsilon_0=0.01$  a.u. at 100 and 200 eV energies for no-photon ( $l=0$ ) exchange.  $x[y]=x \times 10^y$ .

Energy (eV)	Scattering angle (deg)	Differential cross sections							
		$\epsilon_0 \parallel \mathbf{k}_i$				$\epsilon_0 \perp \mathbf{k}_i$			
		$\left[ \frac{d\sigma}{d\Omega} \right]_{100}$		$\left[ \frac{d\sigma}{d\Omega} \right]_{001}$		$\left[ \frac{d\sigma}{d\Omega} \right]_{100}$		$\left[ \frac{d\sigma}{d\Omega} \right]_{001}$	
		No dressing	Dressing	No dressing	Dressing	No dressing	Dressing	No dressing	Dressing
100	0	3.671[+1]	2.709[+1]	0	0	4.431[-1]	3.446[-1]	4.943[+1]	4.943[+1]
	2	1.820[+1]	1.350[+1]	6.977	6.672	8.857	6.791	2.172[+1]	2.136[+1]
	4	5.185	3.901	7.155	6.825	6.310	4.487	4.150	3.859

TABLE III. (Continued).

		Differential cross sections							
		$\epsilon_0 \parallel \mathbf{k}_i$				$\epsilon_0 \perp \mathbf{k}_i$			
Energy (eV)	Scattering angle (deg)	$\left[ \frac{d\sigma}{d\Omega} \right]_{100}$		$\left[ \frac{d\sigma}{d\Omega} \right]_{001}$		$\left[ \frac{d\sigma}{d\Omega} \right]_{100}$		$\left[ \frac{d\sigma}{d\Omega} \right]_{001}$	
		No dressing	Dressing	No dressing	Dressing	No dressing	Dressing	No dressing	Dressing
100	6	1.722	1.320	4.358	4.140	1.938	1.148	6.191[-1]	5.058[-1]
	8	7.291[-1]	5.690[-1]	2.410	2.276	2.761[-1]	8.784[-2]	5.553[-2]	2.990[-2]
	10	3.690[-1]	2.913[-1]	1.296	1.213	4.614[-5]	3.263[-2]	6.782[-6]	2.183[-3]
	12	2.055[-1]	1.632[-1]	6.810[-1]	6.304[-1]	7.167[-2]	1.297[-1]	8.469[-3]	1.384[-2]
	14	1.179[-1]	9.396[-2]	3.466[-1]	3.162[-1]	1.162[-1]	1.410[-1]	1.178[-2]	1.412[-2]
	16	6.647[-2]	5.330[-2]	1.686[-1]	1.508[-1]	9.190[-2]	8.987[-2]	8.365[-3]	8.369[-3]
	18	3.552[-2]	2.892[-2]	7.699[-2]	6.702[-2]	4.653[-2]	3.698[-2]	3.926[-3]	3.239[-3]
	20	1.733[-2]	1.467[-2]	3.208[-2]	2.685[-2]	1.448[-2]	8.306[-3]	1.159[-3]	6.912[-4]
	25	1.162[-3]	1.930[-3]	1.477[-3]	8.974[-4]	9.475[-4]	2.276[-3]	7.081[-5]	1.653[-4]
	30	1.706[-4]	7.373[-4]	1.548[-4]	2.634[-4]	2.215[-3]	2.246[-3]	1.620[-4]	1.662[-4]
	35	6.550[-4]	7.329[-4]	4.397[-4]	4.845[-4]	2.805[-4]	1.667[-4]	2.049[-5]	1.206[-5]
	40	3.704[-4]	3.846[-4]	1.894[-4]	1.842[-4]	1.806[-5]	4.606[-5]	1.328[-6]	3.268[-6]
	45	5.352[-5]	1.240[-4]	2.135[-5]	1.731[-5]	7.332[-5]	8.135[-5]	5.444[-6]	6.068[-6]
	50	2.279[-6]	4.047[-5]	7.223[-7]	1.295[-6]	2.800[-5]	2.410[-5]	2.100[-6]	1.820[-6]
55	1.755[-5]	1.778[-5]	4.486[-6]	4.716[-6]	2.225[-6]	1.152[-6]	1.685[-7]	8.317[-8]	
60	5.720[-5]	1.545[-5]	1.193[-6]	1.057[-6]	3.700[-7]	8.408[-7]	2.826[-8]	5.998[-8]	
200	0	9.315[+1]	7.070[+1]	0	0	4.681[-1]	3.641[-1]	1.073[+2]	1.073[+2]
	2	1.230[+1]	9.443	1.973[+1]	1.931[+1]	1.813[+1]	1.349[+1]	1.075[+1]	1.036[+1]
	4	1.688	1.328	7.895	7.712	3.091	1.861	5.113[-1]	4.242[-1]
	6	5.442[-1]	4.352[-1]	3.114	3.030	1.066[-1]	1.540[-2]	9.241[-3]	2.670[-3]
	8	2.638[-1]	2.114[-1]	1.288	1.246	6.970[-2]	1.441[-1]	4.159[-3]	7.509[-3]
	10	1.430[-1]	1.145[-1]	5.359[-1]	5.142[-1]	1.367[-1]	1.543[-1]	6.522[-3]	7.387[-3]
	12	7.662[-2]	6.141[-2]	2.176[-1]	2.066[-1]	6.663[-2]	5.523[-2]	2.779[-3]	2.388[-3]
	14	3.849[-2]	3.120[-2]	8.418[-2]	7.876[-2]	1.092[-2]	5.161[-3]	4.201[-4]	2.053[-4]
	16	1.756[-2]	1.470[-2]	3.019[-2]	2.768[-2]	3.397[-5]	1.080[-3]	1.248[-6]	3.408[-5]
	18	6.986[-3]	6.349[-3]	9.640[-3]	8.576[-3]	2.898[-3]	4.284[-3]	1.038[-4]	1.537[-4]
	20	2.247[-3]	2.527[-3]	2.534[-3]	2.139[-3]	3.061[-3]	3.154[-3]	1.083[-4]	1.130[-4]
	25	6.935[-7]	3.467[-4]	5.042[-7]	5.109[-6]	7.447[-6]	7.297[-6]	2.626[-7]	9.738[-8]
	30	1.400[-4]	1.726[-4]	7.037[-5]	7.596[-5]	1.150[-4]	1.169[-4]	4.106[-6]	4.203[-6]
	35	5.508[-5]	6.779[-5]	2.011[-5]	1.936[-5]	1.134[-6]	2.819[-7]	4.106[-8]	3.374[-9]
40	9.909[-7]	2.936[-5]	2.724[-7]	1.730[-7]	6.571[-6]	7.167[-6]	2.412[-7]	2.637[-7]	
45	2.848[-6]	5.457[-6]	6.059[-7]	6.480[-7]	8.394[-7]	5.999[-7]	3.116[-8]	2.218[-8]	
50	8.635[-7]	5.051[-6]	1.452[-7]	1.328[-7]	2.140[-7]	2.954[-7]	8.021[-9]	1.088[-8]	
55	1.121[-7]	3.031[-6]	1.514[-8]	1.802[-8]	2.963[-7]	2.910[-7]	1.119[-8]	1.103[-8]	
60	1.561[-7]	8.567[-7]	1.717[-8]	1.633[-8]	3.579[-8]	2.703[-8]	1.360[-9]	1.028[-9]	

TABLE IV. Differential cross sections  $(d\sigma/d\Omega)_{100}$  and  $(d\sigma/d\Omega)_{001}$  ( $a_0^2 \text{ sr}^{-1}$ ) for the excitation of the H atom to the  $n=2$  level under electron impact in the presence of a laser field of strength  $\epsilon_0=0.003$  a.u. at 100 and 200 eV energies for one-photon emission ( $l=+1$ ).  $x[y]=x \times 10^y$ .

		Differential cross sections							
		$\epsilon_0 \parallel \mathbf{k}_i$				$\epsilon_0 \perp \mathbf{k}_i$			
Energy (eV)	Scattering angle (deg)	$\left[ \frac{d\sigma}{d\Omega} \right]_{100}$		$\left[ \frac{d\sigma}{d\Omega} \right]_{001}$		$\left[ \frac{d\sigma}{d\Omega} \right]_{100}$		$\left[ \frac{d\sigma}{d\Omega} \right]_{001}$	
		No dressing	Dressing	No dressing	Dressing	No dressing	Dressing	No dressing	Dressing
100	0	6.396[-1]	9.798[-1]	0	0	0	5.014[-3]	0	0
	2	3.682[-1]	5.659[-1]	1.115[-1]	1.267[-1]	3.702[-2]	1.119[-1]	1.128[-1]	1.284[-1]
	4	1.304[-1]	2.019[-1]	1.438[-1]	1.631[-1]	1.750[-1]	2.462[-1]	1.433[-1]	1.625[-1]
	6	5.208[-2]	8.084[-2]	1.078[-1]	1.219[-1]	2.662[-1]	2.983[-1]	1.049[-1]	1.182[-1]
	8	2.648[-2]	4.062[-2]	7.411[-2]	8.337[-2]	2.844[-1]	2.920[-1]	6.970[-2]	7.783[-2]

TABLE IV. (Continued).

Energy (eV)	Scattering angle (deg)	Differential cross sections							
		$\epsilon_0 \parallel \mathbf{k}_i$				$\epsilon_0 \perp \mathbf{k}_i$			
		$\left(\frac{d\sigma}{d\Omega}\right)_{100}$		$\left(\frac{d\sigma}{d\Omega}\right)_{001}$		$\left(\frac{d\sigma}{d\Omega}\right)_{100}$		$\left(\frac{d\sigma}{d\Omega}\right)_{001}$	
		No dressing	Dressing	No dressing	Dressing	No dressing	Dressing	No dressing	Dressing
100	10	1.653[-2]	2.463[-2]	5.099[-2]	5.703[-2]	2.601[-1]	2.571[-1]	4.591[-2]	5.074[-2]
	12	1.186[-2]	1.695[-2]	3.562[-2]	3.959[-2]	2.176[-1]	2.116[-1]	3.042[-2]	3.323[-2]
	14	9.241[-3]	1.261[-2]	2.523[-2]	2.784[-2]	1.714[-1]	1.657[-1]	2.024[-2]	2.184[-2]
	16	7.520[-3]	9.804[-3]	1.803[-2]	1.975[-2]	1.289[-1]	1.246[-1]	1.347[-2]	1.435[-2]
	18	6.241[-3]	7.808[-3]	1.294[-2]	1.408[-2]	9.337[-2]	9.063[-2]	8.929[-3]	9.389[-3]
	20	5.212[-3]	6.290[-3]	9.313[-3]	1.006[-2]	6.559[-2]	6.400[-2]	5.879[-3]	6.104[-3]
	25	3.275[-3]	3.698[-3]	4.074[-3]	4.328[-3]	2.437[-2]	2.418[-2]	1.989[-3]	2.004[-3]
	30	1.966[-3]	2.130[-3]	1.758[-3]	1.840[-3]	8.068[-3]	8.137[-3]	6.323[-4]	6.205[-4]
	35	1.123[-3]	1.183[-3]	7.460[-4]	7.711[-4]	2.448[-3]	2.508[-3]	1.890[-4]	1.811[-4]
	40	6.125[-4]	6.304[-4]	3.107[-4]	3.177[-4]	6.896[-4]	7.175[-4]	5.306[-5]	4.968[-5]
	45	3.189[-4]	3.205[-4]	1.264[-4]	1.280[-4]	1.798[-4]	1.903[-4]	1.387[-5]	1.265[-5]
	50	1.577[-4]	1.539[-4]	4.974[-5]	4.991[-5]	4.246[-5]	4.589[-5]	3.288[-6]	2.901[-6]
	55	7.319[-5]	6.877[-5]	1.863[-5]	1.852[-5]	8.551[-6]	9.558[-6]	6.654[-7]	5.555[-7]
	60	3.117[-5]	2.806[-5]	6.481[-6]	6.378[-6]	1.244[-6]	1.497[-6]	9.727[-8]	7.146[-8]
200	0	6.848[-1]	1.510	0	0	0	5.355[-3]	0	0
	2	1.239[-1]	2.774[-1]	1.594[-1]	1.815[-1]	2.157[-1]	3.982[-1]	1.590[-1]	1.809[-1]
	4	2.099[-2]	4.783[-2]	8.190[-2]	9.283[-2]	3.891[-1]	4.386[-1]	7.907[-2]	8.924[-2]
	6	8.169[-3]	1.783[-2]	4.153[-2]	4.675[-2]	3.634[-1]	3.652[-1]	3.798[-2]	4.231[-2]
	8	5.101[-3]	1.005[-2]	2.323[-2]	2.592[-2]	2.795[-1]	2.716[-1]	1.969[-2]	2.157[-2]
	10	3.845[-3]	6.734[-3]	1.381[-2]	1.526[-2]	1.924[-1]	1.857[-1]	1.061[-2]	1.141[-2]
	12	3.065[-3]	4.815[-3]	8.475[-3]	9.270[-3]	1.221[-1]	1.182[-1]	5.771[-3]	6.088[-3]
	14	2.457[-3]	3.524[-3]	5.274[-3]	5.712[-3]	7.252[-2]	7.084[-2]	3.110[-3]	3.219[-3]
	16	1.945[-3]	2.593[-3]	3.300[-3]	3.540[-3]	4.077[-2]	4.025[-2]	1.645[-3]	1.671[-3]
	18	1.512[-3]	1.905[-3]	2.066[-3]	2.197[-3]	2.185[-2]	2.181[-2]	8.488[-4]	8.469[-4]
	20	1.155[-3]	1.393[-3]	1.293[-3]	1.364[-3]	1.122[-2]	1.133[-2]	4.260[-4]	4.178[-4]
	25	5.514[-4]	6.197[-4]	3.990[-4]	4.140[-4]	1.773[-3]	1.841[-3]	6.581[-5]	6.190[-5]
	30	2.455[-4]	2.641[-4]	1.230[-4]	1.260[-4]	2.044[-4]	2.201[-4]	7.583[-6]	6.756[-6]
	35	1.035[-4]	1.071[-4]	3.770[-5]	3.824[-5]	1.178[-5]	1.384[-5]	4.393[-7]	3.399[-7]
	40	4.122[-5]	4.056[-5]	1.131[-5]	1.137[-5]	6.853[-8]	3.364[-8]	2.576[-9]	7.722[-9]
	45	1.515[-5]	1.396[-5]	3.219[-6]	3.211[-6]	1.401[-6]	1.274[-6]	5.304[-8]	6.060[-8]
	50	4.914[-6]	4.319[-6]	8.253[-7]	8.161[-7]	1.351[-6]	1.301[-6]	5.144[-8]	5.425[-8]
	55	1.285[-6]	1.379[-6]	1.735[-7]	1.695[-7]	8.078[-7]	7.955[-7]	3.092[-8]	3.161[-8]
	60	2.154[-7]	6.897[-7]	2.366[-8]	2.257[-8]	4.010[-7]	3.996[-7]	1.542[-8]	1.549[-8]

TABLE V. Differential cross sections  $(d\sigma/d\Omega)_{100}$  and  $(d\sigma/d\Omega)_{001}$  ( $a_0^2 \text{sr}^{-1}$ ) for the excitation of the H atom to the  $n=2$  level under electron impact in the presence of a laser field of strength  $\epsilon_0=0.01$  a.u. at 100 and 200 eV energies for one-photon emission ( $l=+1$ ).  $x[y]=x \times 10^y$ .

Energy (eV)	Scattering angle (deg)	Differential cross sections							
		$\epsilon_0 \parallel \mathbf{k}_i$				$\epsilon_0 \perp \mathbf{k}_i$			
		$\left(\frac{d\sigma}{d\Omega}\right)_{100}$		$\left(\frac{d\sigma}{d\Omega}\right)_{001}$		$\left(\frac{d\sigma}{d\Omega}\right)_{100}$		$\left(\frac{d\sigma}{d\Omega}\right)_{001}$	
		No dressing	Dressing	No dressing	Dressing	No dressing	Dressing	No dressing	Dressing
100	0	5.992	8.125	0	0	0	4.980[-2]	0	0
	2	3.437	4.665	1.041	1.157	3.901[-1]	1.036	1.188	1.344
	4	1.205	1.634	1.328	1.471	1.567	1.943	1.284	1.416
	6	4.725[-1]	6.342[-1]	9.781[-1]	1.078	1.797	1.810	7.081[-1]	7.477[-1]
	8	2.338[-1]	3.050[-1]	6.545[-1]	7.161[-1]	1.254	1.198	3.074[-1]	3.033[-1]
	10	1.406[-1]	1.749[-1]	4.338[-1]	4.705[-1]	6.214[-1]	6.015[-1]	1.097[-1]	9.732[-2]
	12	9.604[-2]	1.124[-1]	2.885[-1]	3.095[-1]	2.109[-1]	2.179[-1]	2.947[-2]	2.157[-2]

TABLE V. (Continued).

Energy (eV)	Scattering angle (deg)	Differential cross sections							
		$\epsilon_0 \parallel \mathbf{k}_i$				$\epsilon_0 \perp \mathbf{k}_i$			
		$\left[ \frac{d\sigma}{d\Omega} \right]_{100}$		$\left[ \frac{d\sigma}{d\Omega} \right]_{001}$		$\left[ \frac{d\sigma}{d\Omega} \right]_{100}$		$\left[ \frac{d\sigma}{d\Omega} \right]_{001}$	
		No dressing	Dressing	No dressing	Dressing	No dressing	Dressing	No dressing	Dressing
100	14	7.017[-2]	7.695[-2]	1.915[-1]	2.031[-1]	3.676[-2]	4.563[-2]	4.342[-3]	1.805[-3]
	16	5.258[-2]	5.403[-2]	1.260[-1]	1.319[-1]	6.154[-5]	1.908[-3]	6.433[-6]	2.438[-4]
	18	3.931[-2]	3.796[-2]	8.153[-2]	8.410[-2]	9.034[-3]	6.729[-3]	8.640[-4]	1.684[-3]
	20	2.878[-2]	2.620[-2]	5.143[-2]	5.221[-2]	1.777[-2]	1.564[-2]	1.593[-3]	2.078[-3]
	25	1.103[-2]	8.754[-3]	1.373[-2]	1.328[-2]	6.771[-3]	7.614[-3]	5.525[-4]	4.462[-4]
	30	2.713[-3]	1.933[-3]	2.426[-3]	2.176[-3]	2.844[-5]	1.423[-4]	2.229[-6]	1.146[-6]
	35	2.243[-4]	2.969[-4]	1.490[-4]	1.052[-4]	4.385[-4]	3.750[-4]	3.386[-5]	4.330[-5]
	40	2.366[-5]	1.949[-4]	1.200[-5]	1.969[-5]	2.241[-4]	2.417[-4]	1.725[-5]	1.536[-5]
	45	1.033[-4]	1.329[-4]	4.094[-5]	4.384[-5]	1.398[-5]	2.187[-5]	1.078[-6]	4.480[-7]
	50	4.581[-5]	4.026[-5]	1.445[-5]	1.346[-5]	5.288[-6]	3.595[-6]	4.095[-7]	7.106[-7]
	55	1.468[-6]	2.427[-5]	3.737[-7]	1.950[-7]	1.192[-5]	1.117[-5]	9.279[-7]	1.029[-6]
	60	4.106[-6]	1.504[-5]	8.536[-7]	9.882[-7]	6.248[-6]	6.502[-6]	4.886[-7]	4.608[-7]
200	0	7.010	1.366[+1]	0	0	0	5.320[-2]	0	0
	2	1.264	2.490	1.626	1.831	2.139	3.472	1.576	1.768
	4	2.118[-1]	4.185[-1]	8.265[-1]	9.257[-1]	2.699	2.738	5.485[-1]	5.820[-1]
	6	8.087[-2]	1.499[-1]	4.111[-1]	4.565[-1]	1.299	1.242	1.357[-1]	1.292[-1]
	8	4.900[-2]	8.023[-2]	2.231[-1]	2.450[-1]	3.159[-1]	3.242[-1]	2.225[-2]	1.684[-2]
	10	3.534[-2]	5.032[-2]	1.270[-1]	1.376[-1]	1.775[-2]	2.647[-2]	9.788[-4]	1.957[-4]
	12	2.648[-2]	3.304[-2]	7.322[-2]	7.824[-2]	8.409[-3]	5.830[-3]	3.976[-4]	9.031[-4]
	14	1.949[-2]	2.160[-2]	4.184[-2]	4.405[-2]	2.294[-2]	2.083[-2]	9.838[-4]	1.194[-3]
	16	1.375[-2]	1.371[-2]	2.332[-2]	2.416[-2]	1.407[-2]	1.487[-2]	5.679[-4]	5.190[-4]
	18	9.156[-3]	8.309[-3]	1.251[-2]	1.275[-2]	3.330[-3]	4.319[-3]	1.293[-4]	7.846[-5]
	20	5.694[-3]	4.719[-3]	6.372[-3]	6.385[-3]	5.029[-5]	2.327[-4]	1.909[-6]	6.843[-7]
	25	1.145[-3]	7.919[-4]	8.284[-4]	7.858[-4]	5.666[-4]	5.665[-4]	2.103[-5]	2.121[-5]
	30	6.354[-5]	1.210[-4]	3.183[-5]	2.581[-5]	1.231[-6]	6.384[-6]	4.566[-8]	1.672[-8]
	35	9.047[-6]	6.396[-5]	3.294[-6]	4.111[-6]	2.721[-5]	2.649[-5]	1.015[-6]	1.061[-6]
	40	1.524[-5]	1.403[-5]	4.181[-6]	4.190[-6]	1.038[-6]	1.618[-6]	3.902[-8]	1.750[-8]
	45	1.077[-6]	1.091[-5]	2.289[-7]	1.872[-7]	1.487[-6]	1.329[-6]	5.628[-8]	6.607[-8]
	50	6.925[-7]	9.527[-6]	1.163[-7]	1.281[-7]	5.982[-7]	6.543[-7]	2.278[-8]	1.999[-8]
	55	3.443[-7]	3.386[-6]	4.647[-8]	4.311[-8]	2.464[-10]	2.176[-9]	9.433[-12]	1.669[-10]
	60	4.253[-8]	4.290[-6]	4.672[-9]	5.566[-9]	8.417[-8]	7.838[-8]	3.236[-9]	3.597[-9]

(2) The perturbation matrix in this case is diagonal with respect to the mutually degenerate unperturbed states. Thus the proper approach for having a correct basis to work with, is the parabolic coordinate representation.

(3) In the soft-photon limit (low laser frequency), the present form of the dressed wave function is supposed to be exact up to first order.

(4) As such, there is no other weak field limit in the present theory (in contrast to the work of Francken *et al.* [4]) except for the fact that the field intensity  $\epsilon_0$  should be small compared to the atomic field ( $\sim 10^9$  V/cm) so that the perturbation theory remains valid for the construction of the dressed wave functions.

(5) The most salient feature implicit in the present method is that one is not required to resort to any closure-type approximation in order to perform the infinite summation (including continuum) occurring in the usual perturbation theory. This is because, in the

present analysis, the infinite summation does not occur at all; instead, the first-order correction to the unperturbed wave function contains a finite number of terms (involving different Laguerre polynomials). Thus it is quite reasonable to claim that the present method is advantageous for the numerical evaluation of the transition amplitudes for different excited levels.

Finally, we would like to comment that the electron-exchange effect can be incorporated in the present theory without any further approximation and this will be done in a future work. Moreover, the present first-order theory can be extended to higher orders for the construction of the dressed excited-state wave functions.

#### ACKNOWLEDGMENT

One of us (M.B.) would like to thank the Council of Scientific and Industrial Research, Government of India, for providing partial financial support.

- [1] N. K. Rahman and F. H. M. Faisal, *J. Phys. B* **11**, 2003 (1978).
- [2] S. Jetzke, J. Broad, and A. Maquet, *J. Phys. B* **20**, 2887 (1987).
- [3] R. S. Pundir and K. C. Mathur, *Z. Phys. D* **1**, 385 (1986).
- [4] P. Francken, Y. Attaourti, and C. J. Joachain, *Phys. Rev. A* **38**, 1785 (1988).
- [5] F. W. Byron Jr., P. Francken, and C. J. Joachain, *J. Phys. B* **20**, 5487 (1987).
- [6] L. D. Landau and E. M. Lifshitz, *Quantum Mechanics (Nonrelativistic Theory)*, 3rd ed. (Pergamon, New York, 1985), Chap. X, p. 289.
- [7] W. Magnus, F. Oberhettinger, and R. P. Soni, *Formulas and Theorems for the Special Functions of Mathematical Physics*, 3rd ed. (Springer, New York, 1966), Chap. V, p. 241.
- [8] L. I. Schiff, *Quantum Mechanics*, 3rd ed. (McGraw-Hill, New York, 1981), Chap. 8, p. 265.
- [9] M. Bhattacharya, C. Sinha, and N. C. Sil, *Phys. Rev. A* **40**, 567 (1989).